Inorganica Chimica Acta 363 (2010) 2574–2583

Contents lists available at ScienceDirect

Inorganica Chimica Acta

journal homepage: www.elsevier.com/locate/ica

Homogeneous green catalysts for olefin oxidation by mono oxovanadium(V) complexes of hydrazone Schiff base ligands

Hassan Hosseini Monfared [a,*], Rahman Bikas [a], Peter Mayer [b]

[a] Department of Chemistry, Zanjan University, Zanjan 45195-313, Islamic Republic of Iran
[b] Fakultät für Chemie und Pharmazie, Ludwig-Maximilians-Universität, München, Butenandtstr. 5-13, Haus D, D-81377 München, Germany

ARTICLE INFO

Article history:
Received 4 November 2009
Received in revised form 11 April 2010
Accepted 22 April 2010
Available online 13 May 2010

Keywords:
Vanadium catalyst
Oxidation
Crystal structure
Aroylhydrazone
Hydrogen peroxide

ABSTRACT

Three mono oxovanadium(V) complexes of tridentate Schiff base ligands [VO(OMe)L^1] (**1**), [VO(OMe)L^2] (**2**) and [VO(OMe)L^3] (**3**) obtained by monocondensation of 3-hydroxy-2-naphthohydrazide and aromatic *o*-hydroxyaldehydes have been synthesized (H_2L^1 = (*E*)-3-hydroxy-*N*′-(2-hydroxy-3-methoxybenzylidene)-2-naphthohydrazide, H_2L^2 = (*E*)-3-hydroxy-*N*′-(2-hydroxybenzylidene)-2-naphthohydrazide and H_2L^3 = (*E*)-*N*′-(5-bromo-2-hydroxybenzylidene)-3-hydroxy-2-naphthohydrazide). The complexes were characterized by spectroscopic methods in the solid state (IR) and in solution (UV–Vis, ^{1}H NMR). Single crystal X-ray analyses were performed with **1** and **2**. The catalytic potential of these complexes has been tested for the oxidation of cyclooctene using H_2O_2 as the terminal oxidant. The effects of various parameters including the molar ratio of oxidant to substrate, the temperature, and the solvent have been studied. The catalyst **2** showed the most powerful catalytic activity in oxidation of various terminal, cyclic and phenyl substituted olefins. Excellent conversions have been obtained for the oxidation of cyclic and bicyclic olefins.

© 2010 Elsevier B.V. All rights reserved.

1. Introduction

The catalytic epoxidation of olefins has been a subject of growing interest in the production of chemicals and fine chemicals since epoxides are key starting materials for a wide variety of products [1,2]. Much effort has been made to develop new active and selective oxidation catalysts for those processes that require an elimination of by-products. This transformation using environmentally benign oxidants like H_2O_2 has aroused much interest because the chemical industry continues to require cleaner oxidation, which is an advance over environmentally unfavored oxidations and a step up from more costly organic peroxides.

Two classes of vanadium enzymes, viz. vanadium-nitrogenases and vanadate-dependent haloperoxidases, have so far been found in nature, and their structures and properties have stimulated the search for structural and functional model compounds [3–8]. The use of oxovanadium complexes in oxidation and oxotransfer catalysis has been noted [9,10]. Alpha-olefin polymerization catalyzed by some vanadium(V) complexes has been reported [11,12]. Moreover, the role of vanadium complexes in catalytically conducted redox reactions [13,14], and potential medicinal applications such as in the treatment of diabetes type I and type II [15] have stimulated the interest in the stereochemistry and reactivity of its coordination compounds. In most cases the active site contains either of these two motifs (VO^{3+} or VO^{2+}) coordinated by oxygen–nitrogen atoms. The strong affinity of these two motifs towards O, N-donor ligand is probably due to their hard acidic nature, and selective stabilization of these two motifs depends upon the basicity of donor atoms.

The remarkable biological activity of acid hydrazides R–CO–NH–NH_2, their corresponding aroylhydrazones, R-CO-NH–N=CH–R′, and the dependence of their mode of chelation with transition metal ions present in the living system have been of significant interest [16,17] The coordination compounds of aroylhydrazones have been reported to act as enzyme inhibitors [18] and are useful due to their pharmacological applications [19]. Aroylhydrazones complexes, on the other hand, seem to be a good candidate for catalytic oxidation studies because of their stability to resist oxidation. Hydrazone ligands can act as bidentate, tridentate or tetradentate ligands depending on the nature of heterocyclic ring substituents attached to the hydrazone unit. These ligands due to their facile keto-enol tautomerization and the availability of several potential donor sites can coordinate to metals. Hydrazides and hydrazones have interesting ligation properties due to presence of several coordination sites. These ligands have a tendency to stabilize the vanadium in its highest oxidation state [20–26].

To continue exploring structural and electronic effects of the ortho and para substituents in the aryloxy ring of the hydrazone ligands on vanadium in [V^VO(ONO)(O)] complexes applied in

* Corresponding author. Tel.: +98 241 5152576; fax: +98 241 5283203.
E-mail address: monfared@znu.ac.ir (H.H. Monfared).

0020-1693/$ - see front matter © 2010 Elsevier B.V. All rights reserved.
doi:10.1016/j.ica.2010.04.046

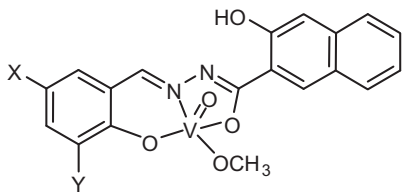

(**1**): X = H, Y = OCH_3
(**2**): X = H, Y = H
(**3**): X = Br, Y = H

Fig. 1. Structural formulae of methoxylatooxovanadium(V) complexes with deprotonated 1:1 condensation products of 3-hydroxy-2-naphthohydrazide with salicylaldehyde and its derivatives.

oxidation catalysis and as part of our research in the study of coordinating capabilities of aroylhydrazones and their coordination compounds [27–31] we report here the synthesis, characterization and efficiency in mediated hydrocarbon oxidation of a series of methoxylato oxovanadium(V) complexes comprising coordinated single condensation products of 3-hydroxy-2-naphthohydrazide with aromatic *o*-hydroxybenzaldehydes along with the X-ray structure analysis carried out on two complexes. Structural formulae of the synthesized catalysts are displayed in Fig. 1.

2. Experimental

Vanadium(IV) oxide acetylacetonate ([$VO(acac)_2$]), olefins, solvents and other materials were purchased in the highest possible purity from Merck and Fluka and used as received. Melting points were recorded on an Electrothermal 9100 apparatus (up to 300 °C). IR spectra were recorded in KBr disks with a Matson 1000 FT-IR spectrophotometer. UV–Vis spectra of solution were recorded on a Shimadzu 160 spectrometer. ^{1}H NMR spectra of ligands in DMSO-d_6 solution were recorded on a Bruker 250 MHz spectrometer and chemical shifts are indicated in ppm relative to tetramethylsilane. The reaction products of oxidation were determined and analyzed by HP Agilent 6890 gas chromatograph equipped with a HP-5 capillary column (phenyl methyl siloxane 30 μm × 320 μm × 0.25 μm) and gas chromatograph–mass spectrometry (Hewlett-Packard 5973 Series MS-HP gas chromatograph with a mass-selective detector). The elemental analyses (carbon, hydrogen, and nitrogen) of compounds were obtained from Carlo ERBA Model EA 1108 analyzer. Vanadium percentages of complexes were measured by a Varian spectrometer AAS-110.

2.1. Synthesis of H_2L^{1-3} ligands

All the three hydrazone ligands (H_2L^{1-3}) were synthesized by the same general method. To a methanol solution (10 ml) of 3-hydroxy-2-naphthohydrazide (1.63 mmol), methanol (10 ml) solution of 2-hydroxybenzaldehyde (1.63 mmol) or its substituted derivatives were drop-wise added and the mixture was refluxed for 3 h. The solution was then evaporated on a steam bath to 5 cm^3 and cooled to room temperature. Yellow crystals of H_2L^{1-3} were separated and filtered off, washed with 5 ml of cooled methanol and then dried in air.

2.1.1. (E)-3-hydroxy-N′-(2-hydroxy-3-methoxybenzylidene)-2-naphthohydrazide (H_2L^1)

Yield 0.54 g (98%). Mp (dp) 297 °C. *Anal.* Calc. for $C_{19}H_{16}N_2O_4$ (MW = 336.34): C, 67.85; H, 4.79; N, 8.33. Found: C, 67.80; H, 4.8; N, 8.43%. IR (KBr, cm^{-1}): 3462 (w, br) ($\bar{\nu}_{O-H}$) 3169 (s,vb) ($\bar{\nu}_{N-H}$), 3085 (s, br), 2946 (m), 1654 (vs) ($\bar{\nu}_{C=O}$), 1615 (m) ($\bar{\nu}_{C=N}$), 1562 (vs), 1469 (s), 1362 (s), 1262 (vs), 1231 (s), 1100 (m), 977 (w), 892 (w), 731 (m), 623 (m), 515 (w), 477 (w). UV–Vis spectrum in CH_3OH [λ_{max}, (ε, M^{-1} cm^{-1})]: 225 (59 850), 290^{sh} (27 200), 313 nm (36 250). ^{1}H NMR DMSO-d_6 (ppm): 12.123 (1H, s) (N–H), 11.250 (1H, s) (aryl-OH), 10.866 (naphthyl-OH), 8.672 (1H, s) (azomethine), 8.473 (1H, s) (naphthyl-3-H), 6.837–7.915 (8H, m) (aromatic), 3.812 (3H, s) (OCH_3).

2.1.2. (E)-3-hydroxy-N′-(2-hydroxybenzylidene)-2-naphthohydrazide (H_2L^2)

Yield 0.475 g (95%). Mp (dp) 317 °C. *Anal.* Calc. for $C_{18}H_{14}N_2O_3$ (MW = 306.32): C, 70.58; H, 4.61; N, 9.15. Found: C, 70.57; H, 4.64; N, 9.18%. IR (KBr, cm^{-1}): 3469 (w, br) ($\bar{\nu}_{O-H}$), 3346 (w, br, $\bar{\nu}_{O-H}$), 3192 (vs) ($\bar{\nu}_{N-H}$), 3031 (vs, vbr), 2669 (m), 2546 (m), 2392 (m, br), 1653 (vs) ($\bar{\nu}_{C=O}$), 1631 (s) ($\bar{\nu}_{C=N}$), 1561 (vs), 1453 (s), 1362 (s), 1277 (vs), 1223 (s), 1169 (m), 1077 (m), 762 (s), 646 (m), 477 (s). UV–Vis spectrum in CH_3OH [λ_{max}, (ε, M^{-1} cm^{-1})]: 237 (62 000), 286 (17 900), 306^{sh} (13600), 338 nm (12800). ^{1}H NMR DMSO-d_6 (ppm): 12.140 (1H, s) (N-H), 11.211 (2H, s) (OH), 8.667 (1H, s) (azomethine), 8.445 (1H, s) (naphthyl-3-H), 6.894-7.917 (9H, m) (aromatic).

2.1.3. (E)-N′-(5-bromo-2-hydroxybenzylidene)-3-hydroxy-2-naphthohydrazide (H_2L^3)

Yield 0.60 g (96%). Mp (dp) 336 °C. *Anal.* Calc. for $C_{18}H_{13}BrN_2O_3$ (MW = 385.21): C, 56.12; H, 3.40; N, 7.27. Found: C, 56.10; H, 3.45; N, 7.30%. IR (KBr, cm^{-1}): 3662 (w, br) ($\bar{\nu}_{O-H}$), 3189 (s, vbr) ($\bar{\nu}_{N-H}$), 3062 (m, br), 1647 (vs) ($\bar{\nu}_{C=O}$), 1625 (m) ($\bar{\nu}_{C=N}$),1552 (s), 1520 (m),1472 (m), 1352 (s), 1268 (vs), 1115 (m), 940 (w), 868 (w), 740 (s), 629 (s), 468 (m). UV–Vis spectrum in CH_3OH [λ_{max}, (ε, M^{-1} cm^{-1})]: 231 (34 350), 287 (10 800), 296^{sh} (10 200), 308 (10 100) 346 nm (7 750). ^{1}H NMR DMSO-d_6 (ppm): 11.953 (1H, s) (N–H), 11.257 (2H, s) (OH), 8.611 (1H, s) (azomethine), 8.419 (1H, s) (naphthohydrazide 3-H), 6.678-7.907 (8H, m) (aromatic).

2.2. Synthesis of the complexes [$V^VO(OCH_3)(L)$] (1–3)

These complexes were synthesized by the same general method. General procedure: The appropriate ligand (H_2L^1, H_2L^2, or H_2L^3) (1.2 mmol) was dissolved in methanol (10 ml). [$VO(acac)_2$] (0.24 g, 1.2 mmol) was added and the solution was gently refluxed for 4 h. After cooling, the resulting solid was filtered off, washed with cooled absolute ethanol, recrystallized from methanol/ethanol (50:50 v/v) and then dried at 100 °C.

2.2.1. [$V^vo(och_3)(l^1)$] (**1**)

Yield 0.44 g (85%). *Anal.* Calc. for $C_{20}H_{17}N_2O_6V$ (MW = 432.30): C, 55.57; H, 3.96; N, 6.48; V, 11.78. Found: C, 55.55; H, 3.96; N, 6.46; V, 11.81%. IR (KBr, cm^{-1}): 3422 (w, br) ($\bar{\nu}_{O-H}$), 2967 (m, br), 2924 (m), 2858 (m), 1638 (s) 1598 (vs), 1573 (m), 1524 (vs), 1465 (m), 1438 (m), 1380 (m), 1340 (s), 1304 (s), 1272 (m), 1240 (m), 1215 (s), 1173 (m), 1035 (s), 997 (vs, V=O), 908 (s), 870 (m), 817 (w), 761 (s), 670 (w), 640 (s), 476 (m). UV–Vis spectrum in CH_3OH [λ_{max}, (ε, M^{-1} cm^{-1})]: 203 (45 600), 230 (39 900), 268^{sh} (24 150), 318 nm (20 200). ^{1}H NMR DMSO-d_6 (ppm): 11.253 (1H, s) (O–H), 9.092 (1H, s) (naphthohydrazide, 3-H), 8.468 (1H, s) (azomethine), 6.852-7.982 (8H, m) (aromatic), 3.782 (3H, s) (aryl-OCH_3), 3.148 (3H, s) (V–OCH_3)

2.2.2. [$V^vo(och_3)(l^2)$] (**2**)

Yield 0.41 g (86%). *Anal.* Calc. for $C_{19}H_{15}N_2O_5V$ (MW = 402.27): C, 56.73; H, 3.76; N, 6.96; V, 12.66. Found: C, 56.74; H, 3.77; N, 6.92; V, 12.70%. IR (KBr, cm^{-1}): 3421 (w,vb), 3011 (m, b), 2954 (m, b), 2908 (m, b), 2808 (m, b), 1636 (s) 1595 (vs), 1548 (m), 1514 (vs), 1462 (s, b), 1382 (m), 1335 (m), 1297 (s), 1217 (s), 1146 (m), 997 (vs, V=O), 987 (s), 898 (m), 865 (w), 836 (w), 800

(w), 762 (s), 695 (w), 634 (vs), 571 (m), 468 (m). UV–Vis spectrum in CH_3OH [λ_{max}, (ε, M^{-1} cm^{-1})]: 203 (45 550), 227 (53 800), 267^{sh} (40 100), 326 nm (33 150). ^1H NMR DMSO-d_6 (ppm): 11.254 (1H, s) (O–H), 9.106 (1H, s) (naphthohydrazide, 3-H), 8.464 (1H, s) (azomethine), 6.817–7.977 (9H, m) (aromatic), 3.142 (3H, s) (V–OCH_3).

2.2.3. [$V^v o(och_3)(l^3)$] (**3**)

Yield 0.47 g (82%). *Anal.* Calc. for $C_{19}H_{14}BrN_2O_5V$ (MW = 481.17): C, 47.43; H, 2.93; N, 5.82; V, 10.59. Found: C, 47.40; H, 3.00; N, 5.85; V, 10.55%. IR (KBr, cm^{-1}): 3415 (w, b), 2913 (w, b), 2858 (w, b), 2805 (m, b), 1637 (s) 1600 (vs), 1534 (s), 1461 (s), 1273 (s), 1215 (s), 1144 (m), 1073 (s), 1034 (m), 999 (vs, V=O), 960 (w), 823 (s), 750 (s), 695 (w), 665 (w), 572 (m), 478 (m). UV–Vis spectrum in CH_3OH [λ_{max}, (ε, M^{-1} cm^{-1})]: 203 (31 350), 226 (46 150), 266^{sh} (36 650), 310^{sh} (28 000), 329 nm (29 100). ^1H NMR DMSO-d_6 (ppm): 11.211 (1H, s) (O–H), 9.073 (1H, s) (naphthohydrazide, 3-H), 8.468 (1H, s) (azomethine), 6.784–7.980 (8H, m) (aromatic), 3.141 (3H, s) (V-OCH_3).

2.3. X-ray Crystallography

X-ray quality crystals of [$V^VO(OCH_3)(L^1)$] (**1**) and [$V^VO(OCH_3)$-(L^2)] (**2**) could be grown from methanol and methanol–acetonitrile (50:50, v/v), respectively. Dark brown crystals of **1** (0.29 mm × 0.07 mm × 0.02 mm) and **2** (0.43 mm × 0.29 mm × 0.16 mm) were investigated in diffraction experiments at 200(2) K on an Oxford XCalibur diffractometer and with monochromated Mo Kα radiation (λ = 0.71073). The structures were solved by Direct Methods with SIR97 [32], and refined with full-matrix least-squares techniques on F^2 with SHELXL-97 [33]. The crystal data and refinement parameters are presented in Table 1. The C-bonded hydrogen atoms were calculated in idealized geometry riding on their parent atoms. The O-bonded hydrogen atoms were located from the difference map and refined freely. The molecular structure plot was prepared using ORTEPIII [34].

Table 1
Crystal data and structure refinement for [$V^VO(OCH_3)(L^1)$] (**1**) and [$V^VO(OCH_3)(L^2)$] (**2**).

	[$V^VO(OCH_3)(L^1)$] (**1**)	[$V^VO(OCH_3)(L^2)$] (**2**)
Net formula	$C_{20}H_{17}N_2O_6V$	$C_{19}H_{15}N_2O_5V$
M_r (g mol^{-1})	432.300	402.274
Crystal system	monoclinic	monoclinic
Space group	$P2_1/c$	$P2_1/n$
a (Å)	14.9240(11)	13.8626(4)
b (Å)	6.3680(4)	8.0484(2)
c (Å)	19.4747(15)	15.4054(5)
α (°)	90	90
β (°)	98.836(8)	101.739(3)
γ (°)	90	90
V ($Å^3$)	1828.8(2)	1682.85(8)
Z	4	4
Calculated density (g cm^{-3})	1.57013(17)	1.58779(8)
μ (mm^{-1})	0.585	0.625
Absorption correction	multi-scan	multi-scan
Transmission factor range	0.98090–1.00000	0.94668–1.00000
Reflections measured	6862	12023
R_{int}	0.0657	0.0226
Mean $\sigma(I)/I$	0.1806	0.0259
θ Range	3.84–25.45	3.78–26.27
Observed reflections	1604	2803
x, y (weighting scheme)	0.0077, 0	0.0472, 0.1170
Reflections in refinement	3338	3407
Parameters	268	249
Restraints	0	0
$R(F_{obs})$	0.0453	0.0285
$R_w(F^2)$	0.0537	0.0826
S	0.735	1.100
Shift/$error_{max}$	0.001	0.001
Max electron density (e $Å^{-3}$)	0.277	0.324
Min electron density (e $Å^{-3}$)	−0.411	−0.304

2.4. Experimental set up for catalytic oxidation

The liquid phase catalytic oxidations were carried out under air (atmospheric pressure) in a 25 ml round bottom flask equipped with a magnetic stirrer and immersed in a thermostated oil bath. In a typical experiment, H_2O_2 (1–4 mmol) was added to a flask containing the catalyst [VO(OMe)L] (2.5×10^{-3} mmol) and a representative olefin, namely cyclooctene (1 mmol) in a solvent (3 ml). The course of the reaction was monitored using a gas chromatograph equipped with a capillary column and a flame ionization detector. The oxidation products were identified by comparing their retention times with those of authentic samples or alternatively by ^1H NMR and GC–Mass analyses. Yields based on the added olefin were determined by a calibration curve. Control reactions were carried out in the absence of catalyst, under the same conditions as the catalytic runs. No products were detected.

3. Results and discussion

3.1. Synthesis of ligands and V-complexes

The reaction of 3-hydroxy-2-naphthohydrazide with several benzaldehyde derivatives containing donor and withdrawing groups in methanol gave the desired dissymmetric tridentate Schiff base ligands in excellent yields and purity (Scheme 1). Vanadium(V) complexes with hydrazone Schiff base ligands were prepared by treating a methanolic solution of the appropriate ligand with an equimolar amount of [$VO(acac)_2$] (Scheme 1).

A list of IR spectral data is presented in Table 2. A comparison of the spectra of the complexes with the ligands provides evidence for the coordination mode of the ligands in the catalysts. The non-observation of the $\bar{\nu}$ (C=O) bands, present in the ligands at 1647–1654 cm^{-1}, indicates the enolization of the amide functionality upon coordination to the V^V-centre. Instead strong bands at ca. 1636–1638 cm^{-1} are observed, which can be attributed to the asymmetric stretching vibration of the conjugated CH=N–N=C group, characteristic for the coordination of the enolate form of the ligands.

On complexation the absence of N–H band, red shifts in azomethine (–C=N–) and carbonyl bands of the ligands show coordination of H_2L^{1-3} as dianionic ligands in enol form (Scheme 1) through the deprotonated hydroxyl group ($O_{phenolate}$), azomethine nitrogen ($N_{azomethine}$) and enol oxygen groups ($O_{O-C(naphthyl)=N}$) in the complexes **1**, **2**, **3** (Table 2). Strong C=N stretch (around 1637 cm^{-1}) indicates the C=N group of the coordinated Schiff base ligands [35]. The strong $\bar{\nu}$ (VO) band around 997 cm^{-1} could be clearly identified for all the complexes.

Methanol solutions of the complexes are brown-yellow in color. These solutions have been used to record the electronic spectra. The hydrazone ligands and their vanadium(V) complexes have bands in the range 203–237 and 318–346 nm (Figs. 2 and 3, Table 3). Based on their extinction coefficients these are assigned as due to $\pi \rightarrow \pi^*$ and $n \rightarrow \pi^*$ transitions, respectively. All bands shift to lower energy in complexes indicating the coordination of ligands to the metal ions. The shoulder at about 270 nm for complexes **1**, **2** and **3** corresponds to LMCT band of V=O which it is seen at 274 nm for [$VO(acac)_2$]. Selected data of ^1H NMR data of the ligands and **1**, **2** and **3** are shown in Table 4. The chemical shifts for the three complexes are comparable and very close to each other.

3.2. X-ray structures of [$V^VO(OCH_3)(L^1)$](**1**) and [$V^VO(OCH_3)(L^2)$] (**2**)

The molecular structures and labeling of the atoms for complexes **1** and **2** are displayed in Figs. 4 and 5, and selected bond

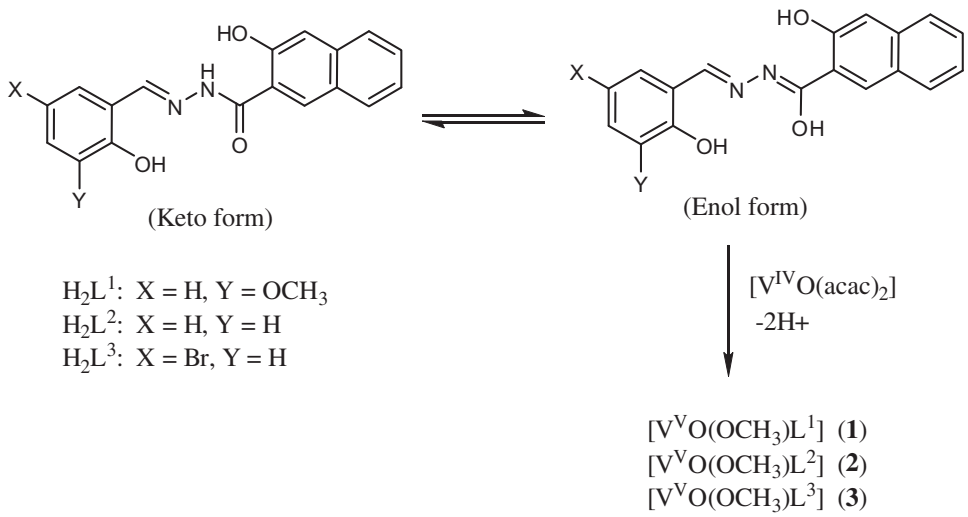

Scheme 1. The syntheses of complexes **1**, **2** and **3**.

Table 2
IR spectral data of the ligands and the vanadium complexes.

Compound	Selected IR bands (cm^{-1})				
	$\bar{\nu}$ (C=N)[a] + δ(NH)	$\bar{\nu}$(C=O)	$\bar{\nu}$(NH)	$\bar{\nu}$(OH)	$\bar{\nu}$ (V=O)
H_2L^1	1615, 1562	1654	3169	3462	
H_2L^2	1631, 1561	1653	3192	3469, 3346	
H_2L^3	1625, 1552	1647	3189	3662	
1	1598	1638		3442	997
2	1595	1636		very broad	997
3	1600	1637		3415	999

[a] The bands assigned to $\bar{\nu}$ (C=N) (azomethyne) may not be pure, as they may be associated with the aromatic (C=C) stretching bands.

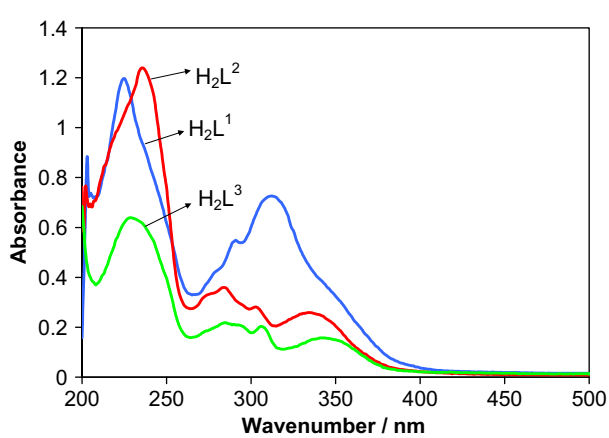

Fig. 2. The UV–Vis spectra of H_2L^1, H_2L^2 and H_2L^3 ($2.0 \times 10^{-5-}$ M) in MeOH.

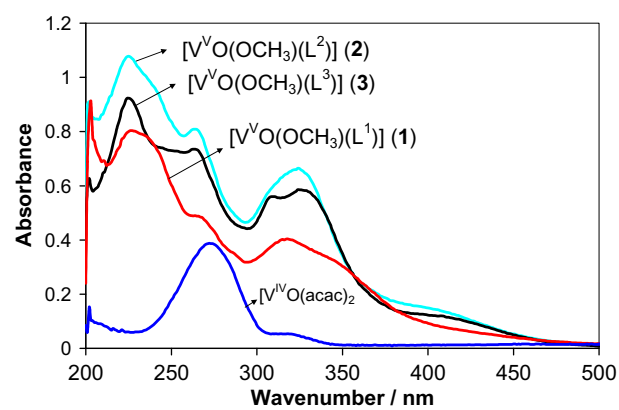

Fig. 3. The UV–Vis spectra of **1**, **2**, **3** and $[VO(acac)_2]$ ($2.0 \times 10^{-5-}$ M) in MeOH.

Table 3
UV-Vis data for **1**, **2**, **3** and $[VO(acac)_2]$ in methanol.

Compound	λ_{max} (nm)/ε (M^{-1} cm^{-1})
H_2L^1	225 (59 850), 290^{sh} (27 200), 313 (36 250)
H_2L^2	237 (62 000), 286 (17 900), 306^{sh} (13600), 338 (12800)
H_2L^3	231 (34 350), 287 (10 800), 296^{sh} (10 200), 308 (10 100) 346 (7 750)
$[VO(acac)_2]$	459 (80) (d–d), 546 (90) (d–d), 274 (19 350)
1	203 (45 600), 230 (39 900), 268^{sh} (24 150), 318 (20 200)
2	203 (45 550), 227 (53 800), 267^{sh} (40 100), 326 (33 150)
3	203 (31350), 226 (46 150), 266^{sh} (36 650), 310^{sh} (28 000), 329 (29 100)

lengths and angles are given in Table 5. In **1** and **2**, the vanadium atom has a five-coordinated structure as a VO(ONO)(O) with nitrogen and two oxygen atoms provided by the Schiff base, an oxygen atom from methoxylato and an oxo ligands. The geometry around the vanadium center in **1** is a square pyramidal with little distortion ($\tau = 0.03$) and remains approximately square pyramidal but the coordination around V in **2** becomes distorted square-pyramidal ($\tau = 0.23$) [36]. The doubly deprotonated Schiff base ligand form a basal plane (O1, N1, O2, O5 for molecules **1** and **2**) through the phenolate oxygen atom O1, imine nitrogen atom N1 and enolate

Table 4
Chemical shifts for the protons of ligands H_2L^1, H_2L^2 and H_2L^3 and complexes **1**, **2** and **3** (δ/ppm).

Compound	–N*H*–	O*H* (aryl)	O*H* (naphthyl)	–C*H*=N–	–OCH_3	V–OCH_3
H_2L^1	12.123	11.250	10.866	8.672	3.812	
H_2L^2	12.140	11.211	11.211	8.667		
H_2L^3	11.953	11.257	11.257	8.611		
1			11.253	8.468	3.782	3.148
2			11.254	8.464		3.142
3			11.211	8.468		3.141

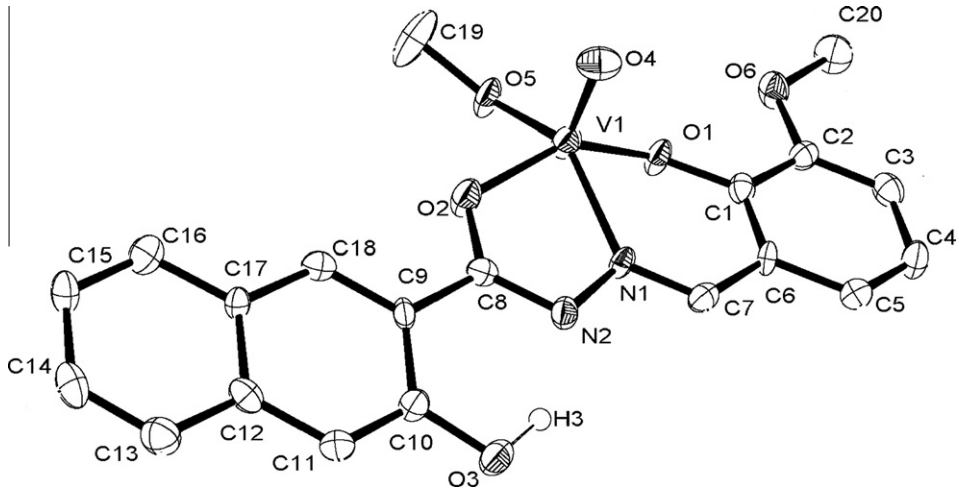

Fig. 4. Thermal ellipsoid plot of $[V^{V}O(OCH_3)(L^1)]$ (**1**) at 50% probability level, bond lengths and angles in Table 5. Hydrogens omitted for clarity.

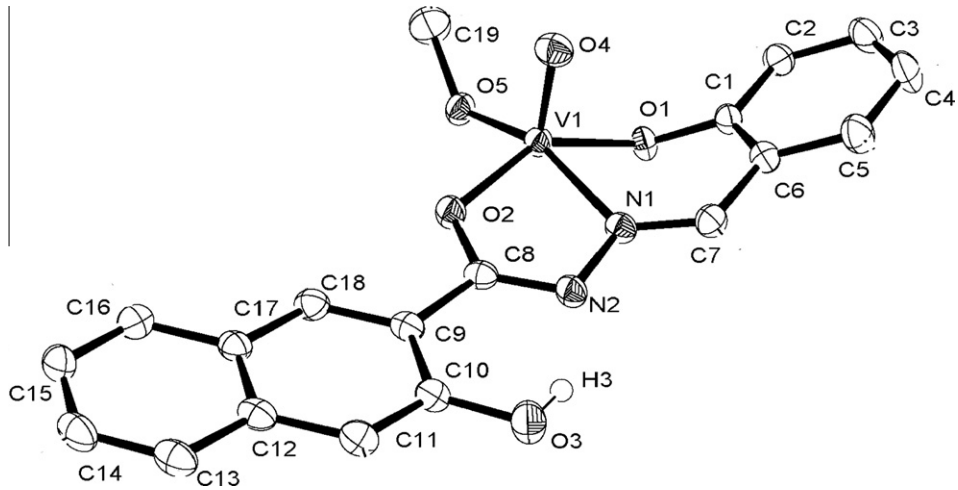

Fig. 5. Thermal ellipsoid plot of $[V^{V}O(OCH_3)(L^2)]$ (**2**) at 50% probability level; bond lengths and angles in Table 5. Hydrogens omitted for clarity.

oxygen atom O2 together with the oxygen atom from the methoxylate ligand The apical position is occupied by the oxo ligand O4. Relative to this plane, the vanadium atom is displaced toward the apical oxygen atom O4 by 0.483(1) and 0.367(1) Å in complexes **1** and **2**, respectively. Moreover, the nitrogen atom N1 of the Schiff base ligand is located *trans* to the methoxylato group O5 with an angle O5–V–N1 of 146.50(10)° in **1** and 160.75(6)° in **2**. The vanadium to terminal oxo group (O4) bond lengths for complexes **1** (1.5758(19) Å) and **2** (1.5857(13) Å) are at the lower end of the typically observed range for oxovanadium(V) complexes [37,38], which is consistent with the reported values of analogous hydrazone complexes [39,40]. The short V–O4 distance indicates the presence of a vanadium–oxygen double bond which is commonly found in the VO^{3+} complexes.

In both compounds the Schiff base ligands form one six-membered and one five-membered chelate ring with bite angles of about 82° (O1–V–N1) and 74° (N1–V–O2), respectively. The double deprotonated form of the N-arylidene naphthohydrazide ligands is consistent with the observed O2–C8 and N2–C8 bond lengths of 1.303(4) Å and 1.310(3) Å, respectively in **1** and 1.316(2) Å and 1.302(2) Å in **2**. This is in agreement with reported titanium and copper complexes containing the enolate form of N-arylidene benzohydrazide ligands [30,31], whereas the O2–C8 bond is considerably short for reported complexes with the coordinated keto form of the *N*-arylidene benzohydrazide system [27]. The vanadium to oxygen bond lengths within the defined tetragonal plane follows the order V–O5 (methoxylato oxygen) < V–O1 (phenolate oxygen) < V–O2 (enolate oxygen). On the other hand, the V–N bond length to nitrogen atom N1 of the Schiff base is considerably elongated due to the *trans* influence of the methoxylato group O5. The oxovanadium(V) complexes reported here crystallize in the monoclinic space groups $P2_1/c$ (**1**) and $P2_1/n$ (**2**) with common structural features. Differences among them can be observed regarding the orientation of the N-arylidene and methoxylato groups. The dihedral angle between vanadium coordinated atoms plane (O1, N1, O2, O5) and *N*-arylidene plane (C1–C6) in **2** is 28.21(7)°, while in **1** is 6.82(13)°.

3.3. Catalytic activity studies

3.3.1. Oxidation of cyclooctene

The catalytic oxidation of cyclooctene with hydrogen peroxide was studied in the presence of $[V^{V}O(OCH_3)(L^2)]$ (**2**). All reactions were carried out with 1 mmol of cyclooctene in CH_3CN and in the presence of 2.5 μmol catalyst at 60 °C temperature for 5 h. Cyclooctene oxide was the sole product. The results of control

Table 5
Selected bond lengths (Å) and angles (°) for **1** and **2**.

1		**2**	
V1–O1	1.834(2)	V1–O1	1.8862(12)
V1–O2	1.944(2)	V1–O2	1.9141(12)
V1–O4	1.576(2)	V1–O4	1.5858(12)
V1–O5	1.741(2)	V1–O5	1.7577(12)
V1–N1	2.108(3)	V1–N1	2.1260(14)
O1–C1	1.338(4)	O1–C1	1.367(2)
O2–C8	1.304(4) (C–O)	O2–C8	1.316(2) (C–O)
O5–C19	1.402(5)	O5–C19	1.414(3)
N1–C7	1.301(4) (N=C)	N1–C7	1.292(2) (N=C)
N1–N2	1.398(4)	N1–N2	1.388(2)
N2–C8	1.310(4) (N=C)	N2–C8	1.302(2) (N=C)
O1–V1–O2	148.14(10)	O1–V1–O2	146.71(5)
O1–V1–O4	105.71(10)	O1–V1–O4	100.68(6)
O1–V1–O5	98.83(10)	O1–V1–O5	100.09(5)
O1–V1–N1	83.06(10)	O1–V1–N1	81.88(5)
O2–V1–O4	100.99(10)	O2–V1–O4	104.28(6)
O2–V1–O5	88.79(10)	O2–V1–O5	95.20(6)
O2–V1–N1	74.13(10)	O2–V1–N1	74.40(5)
O4–V1–O5	108.41(12)	O4–V1–O5	103.44(6)
O4–V1–N1	103.11(11)	O4–V1–N1	94.92(6)
O5–V1–N1	146.50(11)	O5–V1–N1	160.75(5)
V1–O1–C1	134.9(2)	V1–O1–C1	122.64(10)
V1–O2–C8	118.88(19)	V1–O2–C8	119.27(11)
V1–O5–C19	137.1(2)	V1–O5–C19	132.36(12)
V1–N1–C7	128.2(2)	V1–N1–C7	125.56(12)
V1–N1–N2	116.41(19)	V1–N1-N2	115.70(10)

experiments revealed that the presence of catalyst and oxidant are essential for the oxidation. The oxidation of cyclooctene in the absence H_2O_2 does not occur and in the absence of catalyst the oxidation proceeds only up to 6% after 24 h.

In search of suitable reaction conditions to achieve the maximum oxidation of cyclooctene, the effect of oxidant concentration (moles of H_2O_2 per moles of cyclooctene), solvent and temperature of the reaction were studied. The effect of H_2O_2 concentration on the oxidation of cyclooctene is illustrated in Fig. 6. Different H_2O_2/cyclooctene molar ratios (1:1, 2:1, 3:1 and 4:1) were considered while keeping the fixed amount of cyclooctene (1.0 mmol) and catalyst **2** (0.0025 mmol) in 3 ml of acetonitrile at 60 ± 1 °C. Increasing the H_2O_2/cyclooctene ratio from 1:1 to 2:1 increased the conversion from 33 to 90%. Further increment resulted in reduction of conversion. The maximum cyclooctene conversion was obtained with a molar ratio of 2:1.

Fig. 7 illustrates the influence of the solvent nature in the catalytic epoxidation of cyclooctene by **2**. Carbon tetrachloride, methanol, ethanol, acetonitrile, chloroform, tetrahydrofurane (THF), acetone, *N*,*N*′-dimethylformamide (DMF) and ethyl acetate were used as solvents. The highest conversion was obtained in acetonitrile, 92%. It was observed that the catalytic activity of the complex **2** decreases in order acetonitrile (relative dielectric constants [41], $\varepsilon/\varepsilon_0 = 37.5$) > methanol (32.7) > ethanol (26.6) > THF (7.3) > acetone (20.7) > chloroform (4.9) > ethyl acetate (6.0) > CCl_4 (2.24) > DMF (36.7). In Fig. 7, the solvents are shown in order of their

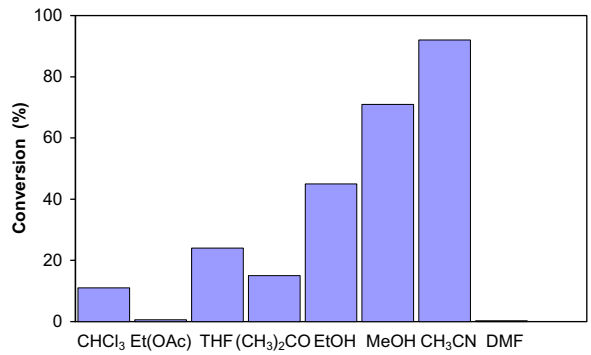

Fig. 7. *Reaction conditions*: catalyst [$V^VO(OCH_3)(L^2)$] (**2**), 2.5 μmol; solvent, 3 ml; cyclooctene, 1 mmol; temperature, 60 °C; aqueous H_2O_2, 2 mmol; the reaction time, 5 h.

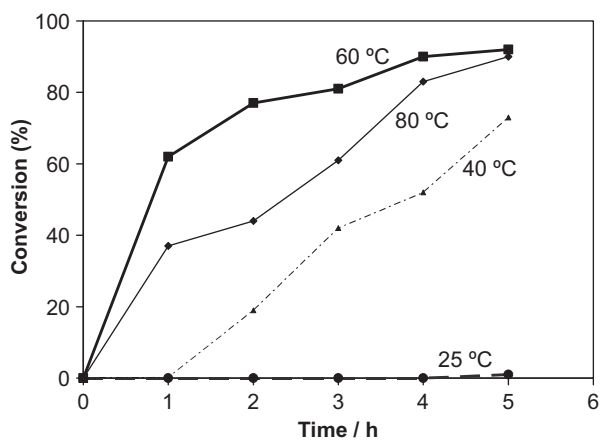

Fig. 8. *Reaction conditions*: catalyst [$V^VO(OCH_3)(L^2)$] (**2**), 2.5 μmol; CH_3CN, 3 ml; cyclooctene, 1 mmol; aqueous H_2O_2, 2 mmol.

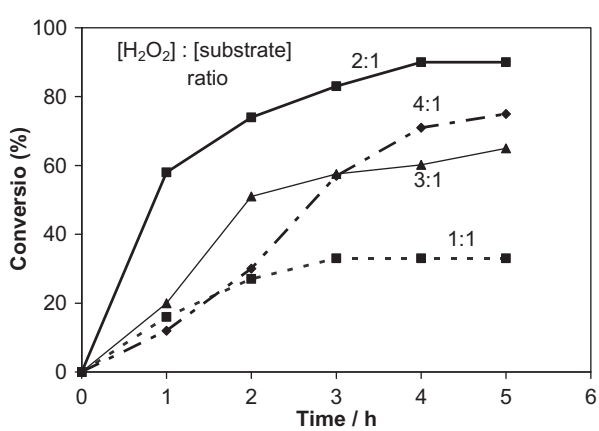

Fig. 6. *Reaction conditions*: Catalyst [$V^VO(OCH_3)(L^2)$] (**2**), 2.5 μmol; CH_3CN, 3 ml; cyclooctene, 1 mmol; temperature, 60 °C; aqueous H_2O_2, 2 mmol.

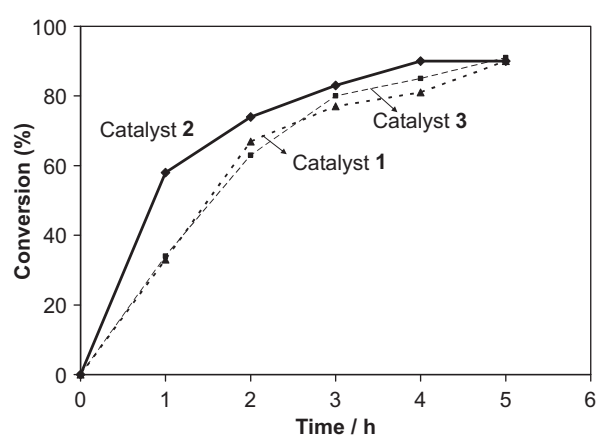

Fig. 9. *Reaction conditions*: catalyst, 2.5 μmol; CH_3CN, 3 ml; cyclooctene, 1 mmol; aqueous H_2O_2, 2 mmol.

Table 6
Oxidation of olefins with $[V^{V}O(OCH_3)(L^2)]$ / H_2O_2 /CH_3CN.

Entry	Olefin	Conversion (%)	Product(s)/yield(s) (%)				
1		90	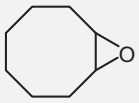	90			
2		92	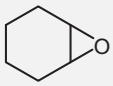	29	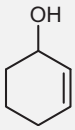	55	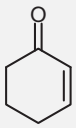 8
3	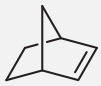	97	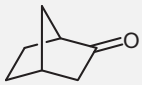	67	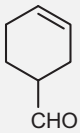	8	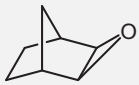 8
				14			
4	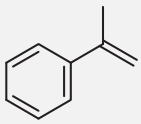	98	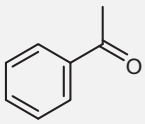	74	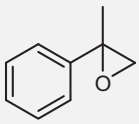	24	
5	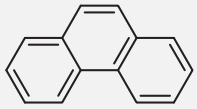	25	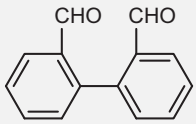	25			
6	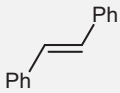	74[a]	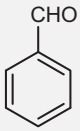	69	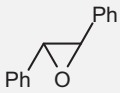	5	
7	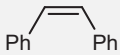	75[a]	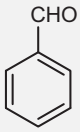	75			

Reaction conditions: catalyst $[VVO(OCH_3)(L^2)]$ (**2**), 2.5 μmol; CH_3CN, 3 ml; cyclooctene, 1 mmol; aqueous H_2O_2, 2 mmol, reaction time, 4 h and temperature, 60 ± 1 °C.
[a] =0.5 mmol. Yields are based on the starting olefin.

relative dielectric constants ($\varepsilon/\varepsilon_0$). In general, there was a good correlation between the solvent polarity ($\varepsilon/\varepsilon_0$) and cyclooctene conversion percent. The highest conversion in acetonitrile possibly is caused by its high dielectric constant. The lowest conversion in DMF is likely due to the highest coordinating ability of DMF (donor number = 24.0[42]). This conclusion was confirmed by the reduction of cyclooctene conversion when the oxidation was carried out in the presence of a co-catalyst imidazole (a good π donor axial ligand). The fine balance between the solvent polarity and its coordinating ability determines its role in the oxidation of cyclooctene by the $[V^{V}O(OCH_3)(L^2)]/H_2O_2$ system.

In order to get the best reaction temperature, the reaction mixture was stirred at various temperatures (for results see Fig. 8). At room temperature the oxidation of cyclooctene was very low. By increasing the reaction temperature the cyclooctene conversion increased and a maximum conversion of cyclooctene (92%) was obtained after 5 h at 60 °C. A temperature rise up to 80 °C lowered the cyclooctene conversion.

The catalytic activities of **1**, **2**, and **3** were examined under the optimized conditions for catalyst **2** (H_2O_2/cyclooctene molar ratio = 2, acetonitrile, reaction temperature 60 °C). Catalyst **1** of shows the lowest and catalyst **2** shows the highest rate of the activity in the oxidation of cyclooctene with H_2O_2 (Fig. 9). Both electron donation and steric effect of ortho methoxy substituent in the aryloxy ring of hydrazone Schiff base ligand decrease the catalytic activity of catalyst **1** relative to catalyst **2**. Since bromo substituent in catalyst **3** is not close to the catalyst active center and also due to its weak electron donation through mesomeric

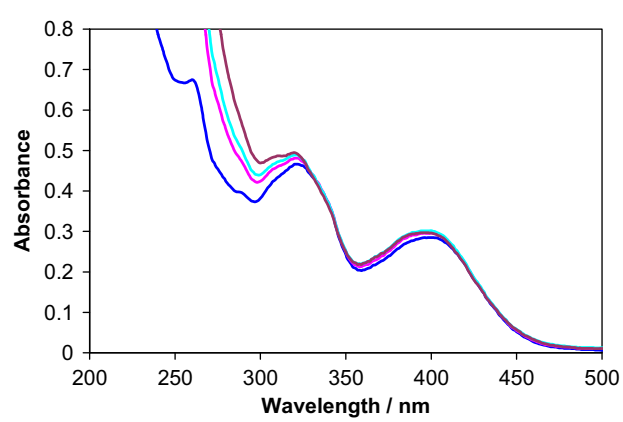

Fig. 10. Titration of $[V^{V}O(OCH_3)(L^2)]$ with H_2O_2. Spectra were recorded after the successive addition of one drop portions of H_2O_2 dissolved in methanol to 5 ml of 3.11×10^{-5} M solution of $[V^{V}O(OCH_3)(L^2)]$.

effect, it slightly decreases the catalyst activity. In general, electronic and steric effects of the ligand substituents are rather subtle since they are far from the reaction center.

3.3.2. Oxidation of various olefins

Finally, in order to explore further the oxidation potential of the hydrazone Schiff base catalyst **2,** oxidation of various olefins was performed under the same reaction conditions which proved to be the best for cyclooctene. We have studied terminal, cyclic and phenyl substituted olefins as substrates. Epoxidation of various olefins by H_2O_2 in the presence of **2** proceeded quantitatively in CH_3CN. This catalytic system led to the oxidation of electron rich olefins, namely, cyclohexene, cyclooctene, norbornene and α-methylstyrene with ⩾90% (Table 6, Entry 1–4). Cyclooctene was converted to the corresponding epoxide with 100% selectivity. For cyclohexene in addition to cyclohexene oxide (29%), allylic oxidation products (2-cyclohexene-1-ol, 55% and 2-cyclohexene-1-one, 8%) were also formed. Allylic oxidation is also seen in the

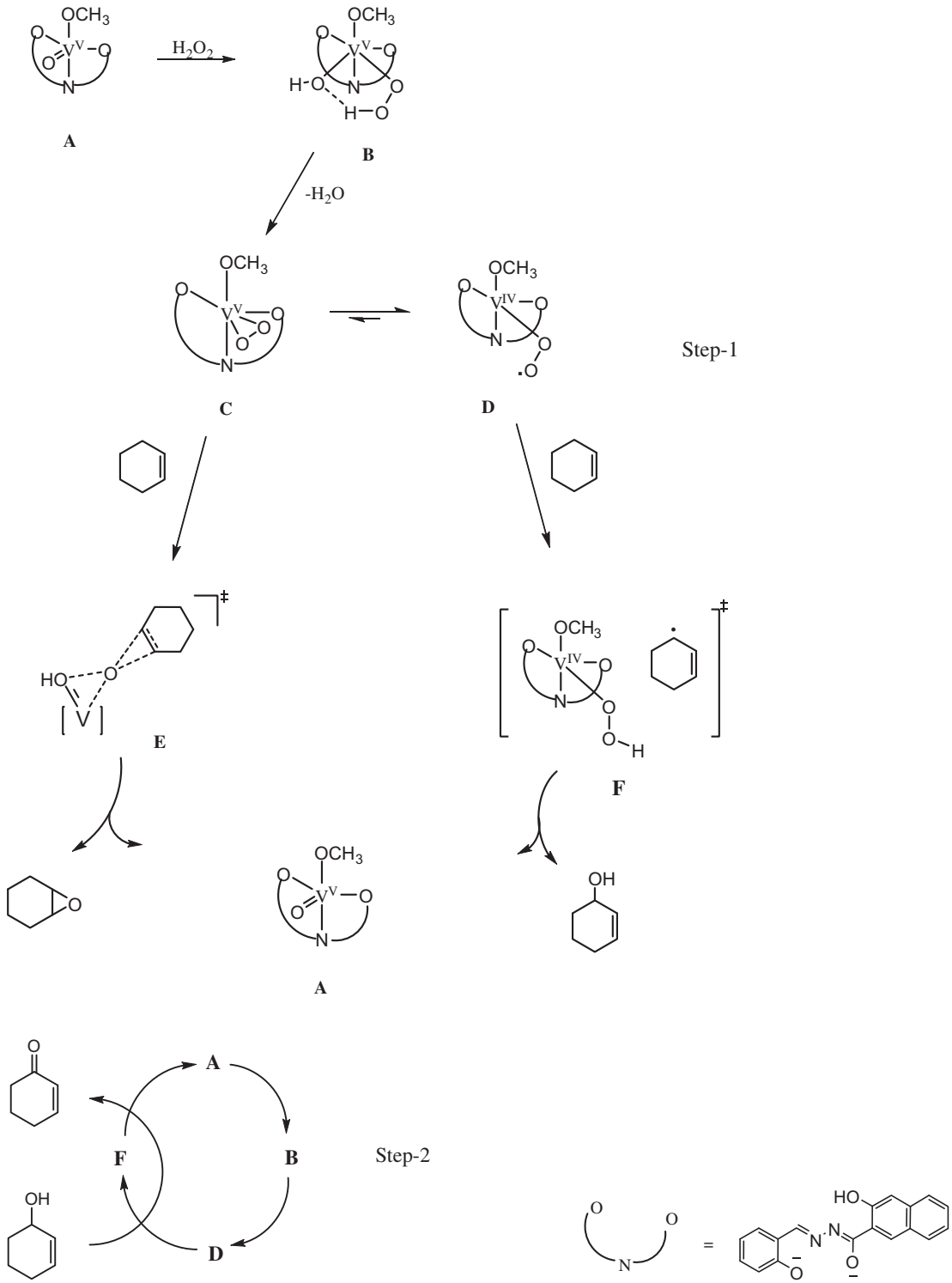

Scheme 2. The proposed catalytic pathway.

metalloporphyrin systems [43,44] in the oxidation of alkenes such as cyclohexene. The oxidation of phenanthrene was proceeded by breaking the double bond and 2,2′-biphenyldicarbaldehyde was the only product. The complex **2** was also tested for the oxidation of *cis*- and *trans*-stilbene where benzaldehyde was obtained as major oxidation product (Table 6, Entry 6 and 7). The presence of electron withdrawing aryl groups on the olefin double bound decreased the conversion percent of the olefin. Phenanthrene and *cis*- and *trans*-stilbene conversion were lower than cyclic and bicyclic olefins and proceeded with the breaking of the double bound. Electron-rich cyclohexene and cyclooctene displayed a greater reactivity than terminal olefins. This reflects the electrophilic nature of the oxygen transfer from the plausible vanadium–oxo intermediate to the olefinic double bond. The higher reactivity of cyclohexene relative to cyclooctene might be due to the greater angle strain in the former. In the oxidation of *cis*- and *trans*-stilbene the steric effects were not distinct. The sterically demanding *trans*-stilbene was a little less reactive than the *cis* isomer. The main product of the oxygenation of *cis*- and *trans*-stilbenes was formed by the breaking of the plausible epoxide and resulted in benzaldehyde.

Overall, activity of the electron rich olefins was higher than the electron poor olefins (phenantheren, *cis*- and *trans*-stilbenes) and there were only relatively small differences in the reactivity of the various electron rich olefins (cyclohexene, cyclooctene, norbornene and α-methylstyrene).

3.4. Possible reaction pathway of the catalysts

In order to establish possible reaction pathway, the methanolic solutions of the neat complex $[V^{V}O(OCH_3)(L^2)]$ were treated with H_2O_2 dissolved in methanol and the progress of the reaction was followed by electronic absorption spectroscopy. Thus, the addition of one-drop portions of 30% H_2O_2 dissolved in methanol to 5 ml of ca. 10^{-5} M solution of $[V^{V}O(OCH_3)(L^2)]$ caused increase in the intensity of 227 nm band and red shift of all bands, Fig. 10. All this suggests the interaction of peroxo group with V(V) center. The observed result is similar to that reported earlier for V=O complexes and is due to the generation of oxomonoperoxovanadium(V) species [45–48]. Peroxovanadium complexes very probably are intermediates in halide oxidation by vanadate-dependent peroxidases, as inferred from the structure results on the peroxo enzyme and by model studies [49]. They are also potential intermediates in the in vitro oxidation reactions of various organic substrates catalysed by vanadium catalyst systems in oxidations carried out with oxygen or peroxides [13].

The total mechanism of the reaction is not fully clear. However, on the basis of the electronic absorption spectroscopy studies and the oxidation products of the various olefins (Table 6), it is predicted that the key step in these processes is the epoxidation of olefins by a peroxo-vanadium-hydrazone Schiff base species formed in the reaction mixture in the presence of hydrogen peroxide. A tentative catalytic pathway for catalytic oxidation of a typical olefin namely cyclohexene is shown in Scheme 2. Cyclohexene is very prone to both allylic and double bond oxidation [43]. The reaction starts from the formation of an active catalytic species $[V^{V}(OO)(OCH_3)(L^2)]$ (Scheme 2, **C**) upon interaction of oxovanadium complex with H_2O_2 which is in equilibrium with a biradical peroxo complex (Scheme 2, **D**). The peroxo complex, thus, transfers one of its oxygen atoms to the substrate in a concerted, highly synchronous attack of the olefin to intermediated **D** [50] and yielding the epoxide and catalyst $[V^{V}(=O)(OCH_3)(L^2)]$. Allylic oxidation of cyclohexene occurs via the vanadium(IV)-peroxo biradical (Scheme 2, **D**) which abstracts a hydrogen atom from the substrate to produce intermediate **F** (Scheme 2). Reduction of the substrate radical by V(IV) gives 2-cyclohexene-1-ol and V(V). The product 2-cyclohexene-1-one is formed in step 2. A similar mechanism has been reported for the catalytic oxidation with oxovanadium(V) complexes of aminebis(phenolate) ligands [51].

In oxidation of α-methyl styrene, phenanthrene, *cis*- and *trans*-stilbene, the high yield of ketone or aldehyde is possibly due to further oxidation of epoxide formed on the first step by the nucleophilic attack of hydroperoxide on epoxide followed by cleavage of the intermediate [48]. The product benzaldehde from further oxidation of styrene is observed by others as well [52].

4. Conclusion

Our work has revealed that coordination complexes of VO^{3+} and tridentate naphthohydrazone Schiff base ligands obtained by reaction of 3-hydroxy-2-naphthohydrazide and aromatic *o*-hydroxyaldehydes derivatives afford a new class of VO^{3+}catalysts for the oxidation of olefins.

Three mono oxovanadium(V) complexes of tridentate Schiff base ligands $[VO(OMe)L^1]$ (**1**), $[VO(OMe)L^2]$ (**2**) and $[VO(OMe)L^3]$ (**3**) were synthezied and characterized by spectroscopic and single crystal X-ray analyses. The catalytic abilities of these complexes were investigated by using the environmentally benign and clean oxidant H_2O_2 for oxidation of olefins. The effects of various parameters including the molar ratio of oxidant to substrate, the temperature, and the solvent have been studied and the optimized conditions were obtained. The catalyst **2** showed the most powerful catalytic activity in oxidation of various olefins. Excellent conversions were obtained for the oxidation of cyclohexene, cyclooctene, norbornene and α-methylstyrene.

Acknowledgments

The authors are grateful to the Zanjan University, the Faculty of Chemistry and Biochemistry of the Ludwig-Maximilians-Universität München, and the School of Chemistry for financial assistance.

Appendix A. Supplementary material

CCDC 748042 and 748043 contain the supplementary crystallographic data for **1** and **2**. These data can be obtained free of charge from The Cambridge Crystallographic Data Centre via www.ccdc.cam.ac.uk/data_request/cif. Supplementary data associated with this article can be found, in the online version, at doi:10.1016/j.ica.2010.04.046.

References

[1] G. Franz, R.A. Sheldon, in: B. Elvers, S. Hawkins, G. Shulz (Eds.), Ullmann's Encyclopedia of Industrial Chemistry, vol. A (18), fifth ed., VCH, Weinheim, 1991, pp. 261–311.
[2] J.T. Lutz, in: M. Grayson, D. Eckroth, G.J. Bushey, C.I. Eastman, A. Klingsberg, L. Spiro (Eds.), Kirk-Othmer Encyclopedia of Chemical Technology, vol. 9, third ed., Wiley, New York, 1980, p. 251.
[3] R.R. Eady, Coord. Chem. Rev. 237 (2003) 23.
[4] M. Weyand, H.-J. Hecht, M. Kiess, M.-F. Liaud, H. Vitler, D. Schomburg, J. Mol. Biol. 293 (1999) 595.
[5] R. Wever, W. Hemrika, in: A. Messerschmidt, R. Huber, T. Poulos, K. Wieghardt (Eds.), Handbook of Metalloproteins, vol. 2, Wiley, Chichester, 2001, p. 1417.
[6] W. Plass, Angew. Chem., Int. Ed. Engl. 38 (1999) 909.
[7] D. Rehder, G. Antoni, G.M. Licini, C. Schulzke, B. Meier, Coord. Chem. Rev. 237 (2003) 53.
[8] D. Rehder, Bioinorganic Vanadium Chemistry, John Wiley and Sons Ltd., 2008.
[9] T. Hirao, M. Mori, Y. Oshiro, J. Org. Chem. 55 (1990) 358.
[10] T. Hirao, T. Fujii, T. Tanaka, Y. Oshiro, J. Chem. Soc., Perkin Trans. 1 (1994) 3.
[11] G.W. Coates, P.D. Hustad, S. Reinartz, Angew. Chem., Int. Ed. Engl. 41 (2002) 2236.
[12] F. Wolff, C. Lorber, R. Choukroun, B. Donnadieu, Inorg. Chem. 42 (2003) 7839.
[13] A. Butler, M.J. Clague, G.E. Meister, Chem. Rev. 94 (1994) 625.
[14] D.C. Crans, J.J. Smee, E. Gaidamauskas, L. Yang, Chem. Rev. 104 (2004) 849.
[15] D.C. Crans, J. Inorg. Biochem. 80 (2000) 123.

[16] L. Savanini, L. Chiasserini, A. Gaeta, C. Pellerano, Bioorg. Med. Chem. 10 (2002) 2193.
[17] J.C. Craliz, J.C. Rub, D. Willis, J. Edger, Nature 34 (1955) 176.
[18] J.R. Dilworth, Coord. Chem. Rev. 21 (1976) 29.
[19] J.R. Merchant, D.S. Clothia, J. Med. Chem. 13 (1970) 335.
[20] A. Pohlmann, S. Nica, T.K.K. Luong, W. Plass, Inorg. Chem. Commun. 8 (2005) 289.
[21] W. Plass, Coord. Chem. Rev. 237 (2003) 205.
[22] S. Nica, A. Pohlmann, W. Plass, Eur. J. Inorg. Chem. (2005) 2032–2036.
[23] R. Dinda, P. Sengupta, S. Ghosh, T.C.W. Mak, Inorg. Chem. 41 (2002) 1684.
[24] T. Ghosh, Transition Met. Chem. 31 (2006) 560.
[25] N.R. Sangeetha, S. Pal, Bull. Chem. Soc. Jpn. 73 (2000) 357.
[26] M.R. Maurya, S. Khurana, C. Schulzke, D. Rehder, Eur. J. Inorg. Chem. (2001) 779–788.
[27] H. Hosseini Monfared, S. Sadighian, M.-A. Kamyabi, P. Mayer, Mol. Catal. A: Chem. 304 (2009) 139.
[28] H. Hosseini Monfared, J. Sanchiz, Z. Kalantari, C. Janiak, Inorg. Chim. Acta 362 (2009) 3791.
[29] O. Pouralimardan, A.–C. Chamayou, C. Janiak, H. Hosseini-Monfared, Inorg. Chim. Acta 360 (2007) 1599.
[30] H. Hosseini Monfared, Z. Kalantari, M.-A. Kamyabi, C. Janiak, Anorg. Allg. Chem. 633 (2007) 1945.
[31] H. Hosseini Monfared, M. Nazari, P. Mayer, M.-A. Kamyabi, A. Erxleben, Z. Asgari, Z. Naturforsch. 64b (2009) 409–414.
[32] A. Altomare, M.C. Burla, M. Camalli, G.L. Cascarano, C. Giacovazzo, A. Guagliardi, A.G.G. Moliterni, G. Polidori, Appl. Crystallogr. 32 (1999) 115.
[33] G.M. Sheldrick, Acta Crystallogr., Sect. A 64 (2008) 112.
[34] L.J. Farrugia, Appl. Crystallogr. 30 (1997) 568.
[35] G. Kolawole, K.S. Patel, J. Chem. Soc., Dalton Trans. (1981) 1241–1245.
[36] A.W. Addison, T.N. Rao, J. Reedijk, J. van Rijnn, G.C. Verschoor, J. Chem. Soc., Dalton Trans. (1984) 1349–1356.
[37] W. Plass, Eur. J. Inorg. Chem. (1998) 799–805.
[38] S. Nica, M. Rudolph, H. Görls, W. Plass, Inorg. Chim. Acta 360 (2007) 1743.
[39] T. Ghosh, S. Bhattacharya, A. Das, G. Mukherjee, M.G.B. Drew, Inorg. Chim. Acta 358 (2005) 989.
[40] B.Mondal, M.G.B. Drew, T. Ghosh, Inorg. Chim. Acta 362 (2009) 3303–3308.
[41] Y. Marcus, in: J. Rydberg, C. Musikas, G.R. Choppin (Eds.), Principles and Practices of Solvent Extraction, Marcel Dekker, New York, 1992, p. 23.
[42] J.E. Huheey, Inorganic Chemistry, third ed., Harper International SI Edition, Cambridge, 1983. p. 340.
[43] D. Mohajer, H. Hosseini Monfared, J. Chem. Res. (1998) 772–773.
[44] A.J. Appleton, S. Evans, J.R. Lindsay Smith, J. Chem. Soc., Perkin Trans. 2 (1995) 281.
[45] T. Joseph, D. Srinivas, C.S. Gopinath, S.B. Halligudi, Catal. Lett. 83 (2002) 209.
[46] C.J. Chang, J.A. Labinger, H.B. Gray, Inorg. Chem. 36 (1997) 5927.
[47] M. Salavati-Niasari, M.R. Elzami, M.R. Mansournia, S. Heidarzadeh, J. Mol. Catal. A: Chem. 221 (2004) 169.
[48] V. Hulea, E. Dumitriu, Appl. Catal. A: Gen. 277 (2004) 99.
[49] G.J. Colpas, B.J. Hamstra, J.W. Kampf, V.L. Pecoraro, J. Am. Chem. Soc. 118 (1996) 3469.
[50] M.L. Kuznetsov, J.C. Pessoa, Dalton Trans. (2009) 5460–5468.
[51] D. Maity, J. Marek, W.S. Sheldrick, H. Mayer-Figge, M. Ali, J. Mol, Catal. A: Chem. 270 (2007) 153.
[52] K. Srinivasan, P. Michaud, J. Am. Chem. Soc. 108 (1986) 2309.